



**HAL**  
open science

## From the very first stages of Mn deposition on Ge(001) to phase segregation

Sion F Olive Mendez, Matthieu Petit, Alain Ranguis, Vinh Le Thanh, Lisa  
Michez

► **To cite this version:**

Sion F Olive Mendez, Matthieu Petit, Alain Ranguis, Vinh Le Thanh, Lisa Michez. From the very first stages of Mn deposition on Ge(001) to phase segregation. *Crystal Growth & Design*, 2018, 18 (9), pp.5124 - 5129. 10.1021/acs.cgd.8b00558 . hal-01902660

**HAL Id: hal-01902660**

**<https://amu.hal.science/hal-01902660>**

Submitted on 23 Oct 2018

**HAL** is a multi-disciplinary open access archive for the deposit and dissemination of scientific research documents, whether they are published or not. The documents may come from teaching and research institutions in France or abroad, or from public or private research centers.

L'archive ouverte pluridisciplinaire **HAL**, est destinée au dépôt et à la diffusion de documents scientifiques de niveau recherche, publiés ou non, émanant des établissements d'enseignement et de recherche français ou étrangers, des laboratoires publics ou privés.



Distributed under a Creative Commons Attribution 4.0 International License

# From the very first stages of Mn deposition on Ge(001) to phase segregation

S. F. Olive Mendez,<sup>†,‡</sup> M. Petit,<sup>†</sup> A. Ranguis,<sup>†</sup> V. Le Thanh,<sup>†</sup> and L.-A. Michez<sup>\*,†</sup>

<sup>†</sup>*Aix-Marseille Univ, CNRS, CINaM, Marseille, France*

<sup>‡</sup>*Present address: Centro de Investigación en Materiales Avanzados, S.C. (CIMA), Av. Miguel de Cervantes No. 120, C.P. 31136 Chihuahua, Chih., Mexico*

E-mail: michez@cinam.univ-mrs.fr

## Abstract

In this work, we have combined scanning tunneling microscopy (STM) with high-resolution transmission electron microscopy (HR-TEM) to investigate the initial stages of Mn deposition on Ge(001) surfaces. The growth temperature has been chosen to be  $(353 \pm 5)$  K, which is typical for the synthesis of  $\text{Ge}_{1-x}\text{Mn}_x$  thin films. At the early stage of the Mn deposition, two distinct kinds of islands are observed even for Mn coverage much smaller than a monolayer with an average size of respectively 1-2 nm and 4-5 nm. Small islands were found to nucleate in the hollow between the Ge dimer rows and they were formed by consuming Ge from two adjacent rows. This indicates that Mn-Ge alloying has been taken place even at the early stage of the Mn deposition. When the Mn coverage increases, coarsening between small islands with newly deposited ad-atoms occurs, giving rise to the formation of monosized islands. Interestingly, these nanostructures have an average size of 4-5 nm and separated by a spacing of 7-8 nm that are similar to the spatial ordering of nanocolumns resulting from spinodal decomposition in (Ge,Mn) thin films. HR-TEM analyses indicate that those

nanoislands are epitaxial, defect free and perfectly coherent with the Ge substrate. A subsequent anneal will result in the formation of  $\text{Mn}_5\text{Ge}_3$  islands.

## Introduction

In the two last decades spintronics has contributed to significant advances in electronics speed and storage and can be used to significantly reduce the energy consumption.<sup>1</sup> However, its more widespread use in microelectronics is hampered by the lack of efficient spin injection.

In recent years, there has been a growing interest in synthesizing diluted magnetic semiconductors (DMS), obtained by substituting  $3d$  transition metal (TM) atoms, such as Mn, Co, Fe, Cr or Ni into non-magnetic semiconductors.<sup>2</sup> Work in this direction has been driven by the hope to significantly improve the efficiency of spin injection into semiconductors. Among the various systems, which have been largely studied, Mn-doped Ge ( $\text{Ge}_{1-x}\text{Mn}_x$ ) is of particular interest since it offers a direct route for integrating magnetism with the existing silicon technology.

One of the major difficulties for getting high-temperature DMS is probably the very low thermodynamic solubility of magnetic transition metal atoms in most semiconductors. It has been estimated to  $10^{-6}$  % for Mn in germanium.<sup>3</sup> As a result, out-of-equilibrium growth techniques, i.e. very low growth temperature, were used to enhance the Mn content up to a few percents. Above this threshold, the formation of Mn-rich phases and/or intermetallic precipitates, mainly  $\text{Mn}_5\text{Ge}_3$ , is generally observed. Park *et al.* demonstrated in DMS thin films grown by molecular beam epitaxy (MBE) at low temperature (343 K) a linear relationship between the Curie temperature and the Mn concentration up to 3.5% corresponding to  $T_C = 116$  K.<sup>4</sup> However, they reported the presence in their films of small Mn-rich precipitates whose concentration did not correspond to any bulk phase. This pioneer work raised the issue of Mn solubility in Ge, even for low Mn concentration and out-of-equilibrium growth. Later, Jamet *et al.* evidenced a novel high-temperature ferromagnetic phase ( $T_C > 400$  K),

whose composition is close to  $\text{Ge}_2\text{Mn}$ . This metastable phase consists of nanocolumns that have an average diameter of 4-5 nm and are separated by a spacing of 10 nm. The formation of these nanocolumns has been attributed to a spontaneous two-dimensional spinodal decomposition taking place at the very early step of the growth<sup>5</sup> but this growth mechanism has not been experimentally confirmed yet. All these experimental findings underline the complexity of the (Ge,Mn) system where Mn diffusion and phase separation prevail. A comprehensive study of the initial growth stage would bring invaluable information on the mechanisms driving the formation of Mn-rich structures.

In a pioneer work, Zeng *et al.* investigated the submonolayer deposition of Mn on Ge(001) as the first step of a subsurfactant epitaxy.<sup>6</sup> They focused on low temperature Mn deposition (150 K), which hampers diffusion leading to Mn trapping at the subsurface interstitial sites. However, such a low temperature is not compatible with a subsequent epitaxial growth. In this work, we report on the first stages of Mn deposition on Ge(001) substrates at  $(353 \pm 5)$  K, corresponding to the substrate temperature typically used for growing  $\text{Ge}_{1-x}\text{Mn}_x$  DMS. Our purpose is to investigate the Mn diffusion process and the phase separation observed during the growth of (Ge,Mn) thin films. Note that this temperature is high enough to allow epitaxial growth but supposedly low enough to limit Mn diffusion and formation of intermetallic precipitates. In order to address this question, we grow some fraction of Mn monolayer (ML) on Ge(001) and use STM, low energy electron diffraction (LEED) and high-resolution transmission electron microscope (HR-TEM) to study Mn adsorption as a function of Mn coverage. In a second part, we will demonstrate that these initial stages of growth of Mn/Ge(001) are determinant for the stabilization of two kinds of GeMn-based nanostructures, namely the nanocolumns and  $\text{Mn}_5\text{Ge}_3$  nanoislands. Both structures have been extensively described in literature. However, their growth mechanisms have not been experimentally evidenced up to now.

# Experimental aspects

Experiments were carried using two connected ultra-high vacuum (UHV) chambers with a base pressure of  $2 \times 10^{-10}$  Torr. In the first chamber, a molecular beam epitaxy (MBE) system is dedicated to Mn and Ge deposition using conventional Knudsen cells. Growth rates have been measured using a quartz crystal microbalance and assessed to be 1.3 and 4.3 ML.min<sup>-1</sup>, respectively. The coverage is given in ML with respect to the unreconstructed Ge(001) surface ( $6.2 \times 10^{14}$  atoms/cm<sup>2</sup>). The second chamber is devoted to surface characterizations with a low-energy electron diffraction (LEED) optics system and a STM microscope, both operating at room temperature. STM measurements were performed in the constant tunneling current mode. The sample during the experiment was grounded, so a bias voltage ( $V_s$ ), typically ranging between -1.5 to 2.0 V, was applied to the tip. High resolution TEM measurements have been performed subsequently using a Jeol 3010 instrument, operated at 300 kV.

The Ge(001) substrates were first chemically cleaned *ex situ*, using a standard procedure so as to remove most of the carbon contaminations as well as the thick GeO<sub>2</sub> superficial native oxide.<sup>7</sup> The sample was annealed *in situ* overnight at  $(773 \pm 5)$  K and then flashed repeatedly at  $(1033 \pm 5)$  K to obtain a  $2 \times 1$  surface reconstruction by LEED. Then 20-nm thick Ge layer was subsequently grown in order to produce a high-quality starting surface: the nearly defect-free surface exhibits long and large terraces (Fig. 1a), mainly constituted of  $2 \times 1$ -reconstructed zone as confirmed by the sharp LEED pattern shown in Fig. 1b and the STM image presented in Fig. 1c. This reconstruction is obtained through the pairing of nearest-neighbor surface atoms forming dimer rows oriented along the  $[1\bar{1}0]$  crystallographic direction.<sup>8</sup> The  $c(4 \times 2)$  mesh, corresponding to out-of-phase buckling of surface dimers, is mainly observed on Ge(001) below 200K.<sup>9</sup> But, as demonstrated in Fig. 1c, this reconstruction can be occasionally observed at room temperature in the vicinity of surface defects where flip-flop motion freezes.<sup>10</sup> The Ge dimers forming zig-zag rows are also oriented along the  $[1\bar{1}0]$  direction. The dimer row direction rotates by 90° from one terrace to the next.

The separation of two adjacent dimers is 4 Å and 8 Å along the  $[1\bar{1}0]$  and  $[110]$  directions, respectively.

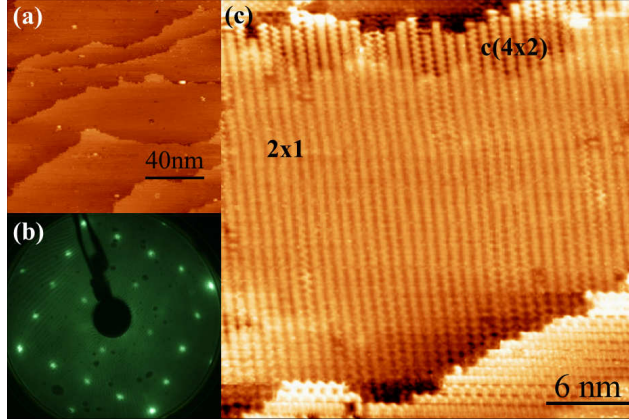


Figure 1: STM images of Ge (001) after the growth of a buffer layer and an anneal at 1033 K. a) Long and large terraces with a width of  $\sim 30$  nm. The sample bias ( $V_s$ ) is -2.2 mV and the current ( $I$ ) is 0.5 nA. b) Very sharp LEED pattern corresponding to the  $2 \times 1$  reconstruction. c) Almost defects free surface with  $V_s = -2.1$  mV;  $I = 0.5$  nA.

## Results and discussion

### Initial stages of Mn adsorption on Ge(001)

This high-quality Ge(001) surface is used as a template to study the initial stage of Mn adsorption. The substrate temperature has been chosen to be  $(353 \pm 5)$  K on Ge(001), which is considered as standard conditions for DMS synthesis.<sup>4,11</sup> Fig. 2a shows a STM image after deposition of  $(0.26 \pm 0.03)$  ML of Mn. The bright contrasts correspond to Mn-induced features. Unlike Mn deposition on Ge(111) for similar growth temperature,<sup>12</sup> the Mn atoms are not randomly distributed on the surface but aggregate to form clusters that are evenly distributed over the terraces. This Volmer-Weber-type growth mode is consistent with the values of surface energy that is higher in Mn than in Ge. The terrace edges do not act as preferential nucleation sites. In our case, two kinds of features can be observed leading to a bimodal size distribution centered on  $(1.4 \pm 0.5)$  nm and  $(3.6 \pm 1.0)$  nm (Fig.

2c) corresponding to a height of  $(2.2 \pm 0.5) \text{ \AA}$  and  $(5.0 \pm 1.0) \text{ \AA}$ , respectively (Fig. 2d). The largest clusters of Fig. 2a appeared to be faceted as shown in Fig. 2b where the facets of specific orientations has been determined through an interactive study of the nanostructures shapes. In this analysis, only clusters with a diameter above 3 nm have been considered. This suggests privileged directions for the nanoislands facets that are mostly perpendicular to the Ge [110], [1-10], [100] and [010] directions. To prevent this clustering phenomenon, low temperature deposition is essential and a growth temperature below 200 K allows to reduce enough surface diffusion resulting in an uniform distribution of Mn atoms trapped in the subsurface interstitial sites  $I_0$ .<sup>6</sup>

A closer study of the small islands brings new insights into the initial Mn clustering process. During this initial stage, the interaction between the Mn and Ge(001) is indeed strong enough to provide well-defined nucleation sites. These features are clearly positioned on the hollow ( $H$ ) sites located in the trench between two Ge dimers of two different rows of the  $2 \times 1$  reconstruction (Fig. 3).

These observations are consistent with the available theoretical assessments of the preferential adsorption of  $3d$ -metals on a surface of Si(001)<sup>13,14</sup> and Ge(001).<sup>15</sup> Calculations have been carried out for a number of high-symmetry adsorption sites that are likely to host  $3d$ -element atoms in diverse systems: Co on Si(001),<sup>14</sup> Mn on Si(001),<sup>13,16-19</sup> Co on Ge,<sup>20</sup> Mn on Ge(001).<sup>15</sup> It has been energetically predicted that the most favorable surface sites are the pedestal ( $P$ ) and the hollow ( $H$ ) sites, as shown in Fig. 3c and Fig. 3d. During the initial growth stage of ad-atoms on Ge(001) or on Si(001), an incoming  $3d$ -transition metal atom may arrive at any of the possible adsorption sites but will diffuse to a more energetically favorable situation. Once it arrives at the  $P$  or  $H$  site, it is unlikely to diffuse along the surface. In the particular case of Mn ad-atoms on Ge(001) surface, it has been found that the  $H$  and  $P$  states are metastable adsorption sites: the total energies of the system for a Mn ad-atom adsorbed at  $H$  or  $P$  have been calculated to be 0.64 and 0.63 eV, respectively.<sup>15</sup> The energy barrier to hop from the  $P$  site to the  $H$  site is assessed to 0.59

eV whereas the migration barrier height for the backward diffusion from the  $H$  site to the  $P$  site is 0.58 eV.<sup>15</sup> A Mn atom can hop from one  $H$  site to another one by overcoming 0.58 eV barrier.<sup>15</sup> As expected, we observe protrusions in the  $H$  sites, their average height is 2.2 Å, which is a bit more than the apparent height of isolated ad-atoms and is not consistent with a single ad-atom on a hollow site ( $H$ ). No Mn atoms have been observed in  $P$  sites. Interestingly, each cluster is bordered by two holes in the Ge surface, which suggests that Mn reacts with Ge atoms to form a primary alloy. Such strong Mn-Ge interactions have been already measured for Mn adsorption on Ge quantum dot {105} facet.<sup>21</sup> Interestingly, no hole in the Ge surface is observed in the latter case. Similarly, Ge-Mn bonding has been theoretically predicted in the case of a single Mn atom in a Ge matrix.<sup>22</sup> This strong interaction is assigned to hybridization between Mn  $d$ -states and Ge  $sp^3$ -band.

Next, we investigate the possibility for the Mn atom to diffuse across the Ge(001) plane into the subsurface. This diffusion process is the precursor of germanidation. In all the calculations performed for adsorption of a 3d-element on Ge(001)<sup>15,20</sup> and on Si(001),<sup>13,14,16,17</sup> the most stable adsorption site is the interstitial site ( $I_0$ ) located under the dimer yielding to the strongest binding for the ad-atoms. In the case on Mn/Si(001), Mn atoms are kinetically limited for diving into the subsurface layer or diffuse into the deep layer at room temperature resulting in an easy diffusion along and across the dimer rows, which leads to the formation of self-assembled Mn atom chains at room temperature.<sup>18,19</sup> This may be attributed to the strong bonding and shorter bond length between Si-Si and Si-Mn on Si(001) (with reference to) in regard to the weak bonding and longer bond length between Ge-Ge and Ge-Mn on Ge(001). This has been experimentally checked for Co on Ge(001),<sup>20,23</sup> Pt or Au on Ge(001)<sup>24</sup> and also for Mn adsorption on Ge(001) when the temperature is low enough to suppress lateral diffusion that causes clustering.<sup>6</sup> In this situation, the Ge dimer in the first layer is lifted away from the subsurface Mn atom and becomes almost symmetric, which facilitates its ejection. Zhu *et al.* have considered the diffusion processes of Mn from the two stable surface adsorption sites, namely,  $P$  and  $H$ , to the subsurface site  $I_0$ . The activation

energies for the Mn atom to diffuse from  $H$  or  $P$  to  $I_0$  are respectively 0.69 eV and 0.59 eV, which is comparable to the calculated barrier heights for surface diffusion.<sup>15</sup> However, the backward diffusion is unlikely to occur as the Mn atom has to overcome an energy barrier of respectively 1.33 eV and 1.22 eV to reach a surface site. Based on the calculated barrier heights for the surface and subsurface diffusion, we note that diffusion of Mn from the Ge(001) surface into the subsurface and surface diffusion are equivalent processes from the energetic point of view. This is consistent with available experimental results of Zeng *et al.*,<sup>6</sup> where it is demonstrated that the surface diffusion has significant contribution to the mass transport of Mn atoms that tend to form clusters at room temperature whereas uniform subsurface adsorption is only observed at 150 K.

A closer study on the STM images sheds new light on the clustering process in Mn/Ge(001) systems: a cluster is nucleated when two dimers from adjacent rows are broken, which is very unusual for  $3d$ - or  $5d$ -element adsorption on Ge(001) or Si(001). This result suggests the presence of an interaction between dimers of adjacent rows, probably mediated by the presence of ad-atom in the  $H$  site, alike to the case of Mn adsorption on Si(001) where it has been predicted that for the two Mn atoms adsorption structures, the most stable configuration is a combination of the  $H$  and  $I_0$  sites. The simultaneous presence of ad-atoms in both a  $H$  and  $I_0$  sites induces the break of the Si dimer.<sup>13</sup> In our system, a  $(I_0)_n + H + (I_0)_{n+1}$  adsorption configuration may be at the origin of the cluster formation where  $(I_0)_n$  and  $(I_0)_{n+1}$  denote  $I_0$  adsorption sites on adjacent dimer rows. Indeed the Mn atom in the  $H$  site cannot dive into the adjacent  $I_0$  subsurface site that are already occupied. This locks the subsurface diffusion process. Subsequently, the ejected Ge atoms react with Mn atoms to form an alloy.

## Mn-induced nanoislands

A progressive increase of Mn coverage to  $(0.52 \pm 0.05)$  ML (Fig. 4a) then to  $(0.65 \pm 0.05)$  ML (Fig. 4b) leads to a decrease of the islands density as illustrated in Fig. 4c where the nanoislands height is plotted as the function of their surface area. Very few protrusions

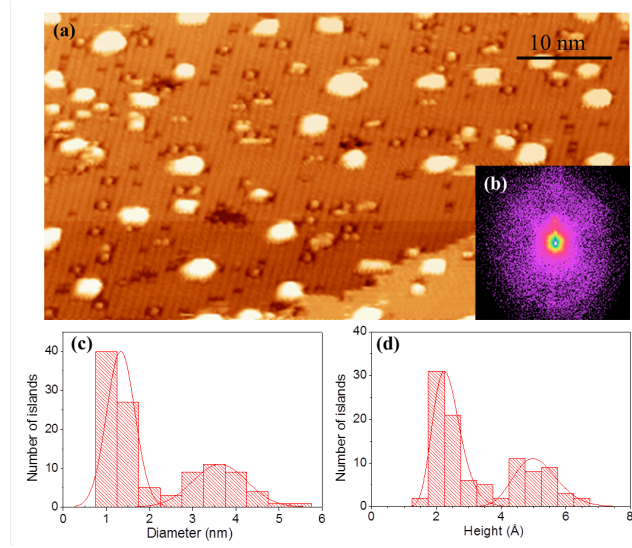


Figure 2: STM images after the deposition of  $(0.26 \pm 0.03)$  ML of Mn on Ge(001) deposited at  $(353 \pm 5)$  K. The sample bias ( $V_s$ ) is 1mV and the current ( $I$ ) is 0.5 nA for all images. a) Mn islands randomly distributed on Ge(001) showing a bimodal distribution of size centered on 1.4 nm and 3.6 nm. b) Facet analysis distribution of Fig. 2a processed by using the software Gwyddion.<sup>25</sup> c) Diameter and d) Height distributions of the nanoislands observed in Fig. 2a.

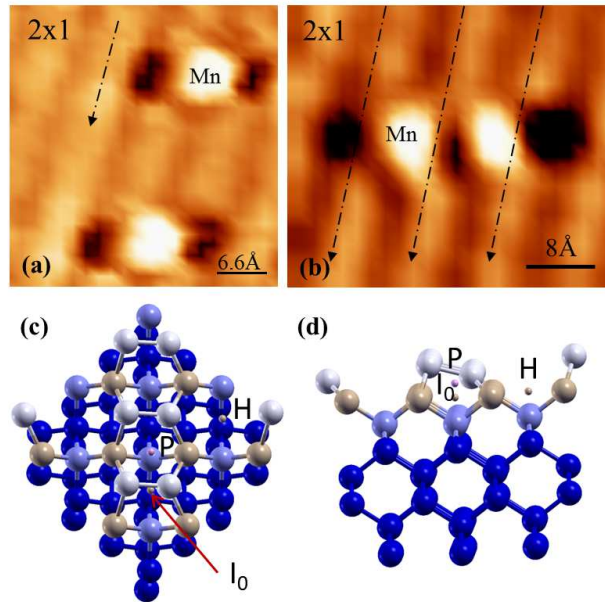


Figure 3: Magnified images of Fig. 2a of: a) and b) two manganese atoms in hollow sites between  $2 \times 1$  rows. c) and d) Top view and side view of a reconstructed Ge(001)- $2 \times 1$  surface showing the hollow  $H$ , pedestal  $P$  and interstitial  $I_0$  adsorption sites. The dimers are constituted by the atoms of the topmost layer drawn in light gray.

corresponding to the initial deposition stage (area of 1-2 nm<sup>2</sup>) are observed in Fig. 4b, probably absorbed to larger islands by Ostwald ripening. This also indicates that the Mn incorporation on already existing clusters is favorable in relation to the formation of new point defects. Furthermore, a higher Mn coverage induced an increase of the height rather than of the diameter (Fig. 4c). This preferential growth indicates that adsorption on Mn-rich islands is energetically more favorable than increasing the island interface with Ge. As a result, islands with almost the same diameter (4-5 nm) self-assemble on the surface with a density of about 32000 islands/ $\mu\text{m}^2$  as shown in Fig. 5a. The average distance between the islands centers is about 10 nm. A cross-sectional HR-TEM image of a typical island is presented in Fig. 5b. Image contrasts can be observed in the Ge wafer in the vicinity of the interface, which indicates the presence of stress in subsurface. This is most probably induced by the epitaxial growth. The presence of Mn in subsurface may be one of the origins. Neither dislocation nor defect is visible at the interface. The islands are perfectly coherent with the substrate. The Fourier transform of the image centered on the island shows that the latter is fully strained on the Ge cubic structure (inset of Fig. 5b).

These results highlight the difficulty of obtaining a uniform Mn distribution on Ge(001) surface. This condition is however a key issue in the perspective of Mn dilution in Ge. The use of an out-of-equilibrium growth technique does not hamper surface diffusion and Mn-Mn interaction, leading to Mn clustering on surface, even at 353 K. Such Mn aggregation has been observed in many works on (Ge,Mn) thin films synthesis with growth temperature varying between room temperature and 573 K and a Mn concentration in the range of 0-10%. It is now well admitted that these growth parameters strongly influence the crystalline quality of the thin films and may cause the formation of secondary phase precipitates. For instance, a growth temperature above 473 K will induce the formation of nanoscale Mn<sub>5</sub>Ge<sub>3</sub><sup>26,27</sup> or Mn<sub>11</sub>Ge<sub>8</sub><sup>4,28</sup> clusters leading to a Curie temperature of 300 K and 285 K, respectively. Lower growth temperature is therefore required to avoid the presence of precipitates, but the formation of Mn-rich zones can still be observed.<sup>29-31</sup>

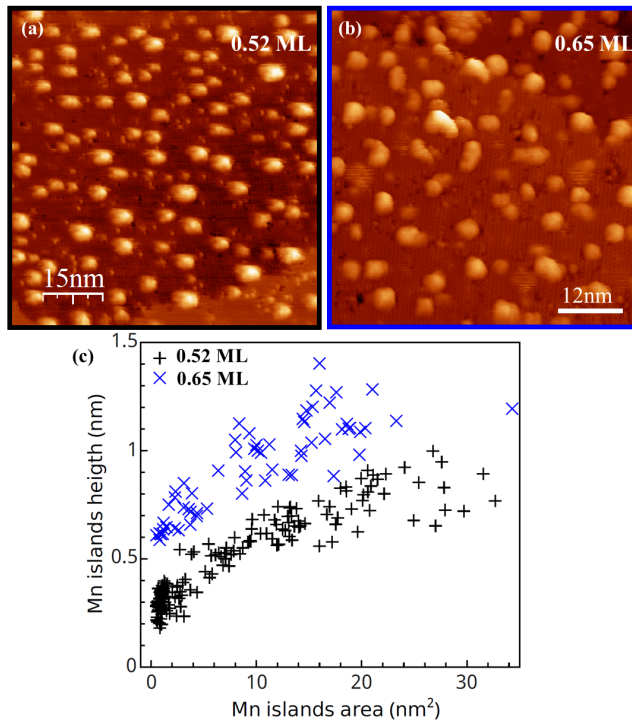


Figure 4: STM images for different Mn deposition a) ( $0.52 \pm 0.05$ ) ML; b) ( $0.65 \pm 0.05$ ) ML ( $V_s = -1.2\text{mV}$ ;  $I = 0.5\text{nA}$ ); Height distribution of the nanoislands as a function of their surface area for the two Mn coverages corresponding to Fig. 4a (black + marks) and Fig. 4a (blue  $\times$  marks).

As a further example, the growth of thin films by codepositing Mn and Ge using specific growth conditions leads to the formation of a columnar Mn-rich phase that is well described in literature.<sup>32-35</sup> To illustrate this point, we present in Fig. 5c the plane-view high-resolution TEM image of a sample containing  $\sim 12$  % Mn. This film has been synthesized by codeposition of Mn and Ge using similar growth conditions (substrate temperature and Mn deposition rate) to the ones used for the nanoislands growth. The nanocolumns that grow perpendicularly to the interface with Ge(001) are uniform in diameter and separated by an average distance of a tenth of nanometers. Remarkably, such structures present the highest Curie temperature reported in the (Ge,Mn) system so far ( $T_C > 400$  K).<sup>32,34</sup> The growth mechanism has been assigned to a spinodal decomposition occurring layer by layer like in (Zn,Cr)Te.<sup>5</sup> Interestingly, Devillers *et al.* have shown that the morphology of the columnar phase is driven by the growth parameters such as the growth temperature ( $T_G$ ) and the Mn concentration.<sup>33</sup> For instance, for a  $T_G$  of 373 K that is close to our experimental conditions, these nanostructures are fully strained in the surrounding Ge matrix and exhibit a cubic structure. Furthermore, their octagonal shapes minimize the interfacial energy.<sup>36</sup> If the columns diameter is not very dependent on the manganese concentration, their density increases greatly with Mn concentration up to a saturation value of  $35000 \mu\text{m}^{-2}$ ,<sup>33</sup> which is comparable with the nanoislands density. Arras *et al.* have identified the  $\alpha$ -Ge<sub>2</sub>Mn-based phase as the best candidate to form the nanocolumns, being both energetically favorable and compatible with experimental findings.<sup>36</sup> In this phase, Mn atoms with a concentration ranging between 20 and 40 % are placed in interstitial position into the single cubic crystal of Ge. This is in agreement with experimental findings.<sup>35</sup> The similarities in spatial distribution, shape and density between the nanoislands (Fig. 5a) and the nanocolumns system (Fig. 5c) are striking apart from the nanoislands diameter. The latter may be larger as Mn diffusion is not hampered by Ge deposition. Our experimental study clearly demonstrates that nanoislands constitute the first stage of the nanocolumnar phase. The fully strained structure probably contains Mn atoms in the interstitial sites of the subsurface. The experi-

mental conditions ( $T_G$ , Mn concentration, slow deposition rates) determine the nanocolumns characteristics (size, density, composition) that result from a competition between chemical, elastic and interfacial energy-terms.<sup>36</sup>

A subsequent anneal of the nanoislands leads to the formation of  $Mn_5Ge_3$  as demonstrated by Olive *et al.*<sup>37</sup> The growth of the  $Mn_5Ge_3$  phase on Ge(001) is remarkable because endotaxial: its interface is buried in the substrate, as shown in Fig. 5d. Indeed, only part of the island emerges from the surface, the rest being buried in the substrate of Ge(001). Its interfaces are coherent with the surrounding Ge matrix. The endotaxial growth has been discovered in the Co/Si(111) system,<sup>38</sup> but also occurs in many other 'TM/Si' structures.<sup>39</sup> It requires the formation of a zone rich in TM element in the subsurface and high annealing temperatures, resulting in significant diffusion of the transition metal into Ge. The existence of privileged adsorption positions in the subsurface interstitial sites of Ge (001) allows the Mn to penetrate into the substrate. Interfaces also play a significant role in the phenomenon of endotaxy. The energy of the interface  $Mn_5Ge_3$  [0001] // Ge [001] is very high (89 meV/Å<sup>2</sup>). As a result, the direct epitaxy of  $Mn_5Ge_3$  on Ge (001) is difficult.<sup>36</sup> This partly explains the shape of the island that tends to minimize the area of this interface.

Our experimental results are in very good agreement with the sequential growth scenario for the nanocolumns formation theoretically proposed by Arras *et al.*<sup>36</sup> The high surface diffusion makes possible the precipitation of Mn-rich domains, probably from the subsurface interstitial sites. These defects act as nuclei for the germination of a coherent phase, the faceted shape of the nanostructures trying to minimize the interface energy. A chemical analysis would be necessary to determine their composition and compare it with the  $\alpha$ - $Ge_2Mn$ -based phase. This metastable phase would eventually transform into the stable and less coherent  $Mn_5Ge_3$  phase thanks to 3D-diffusion, thermally activated in our case.

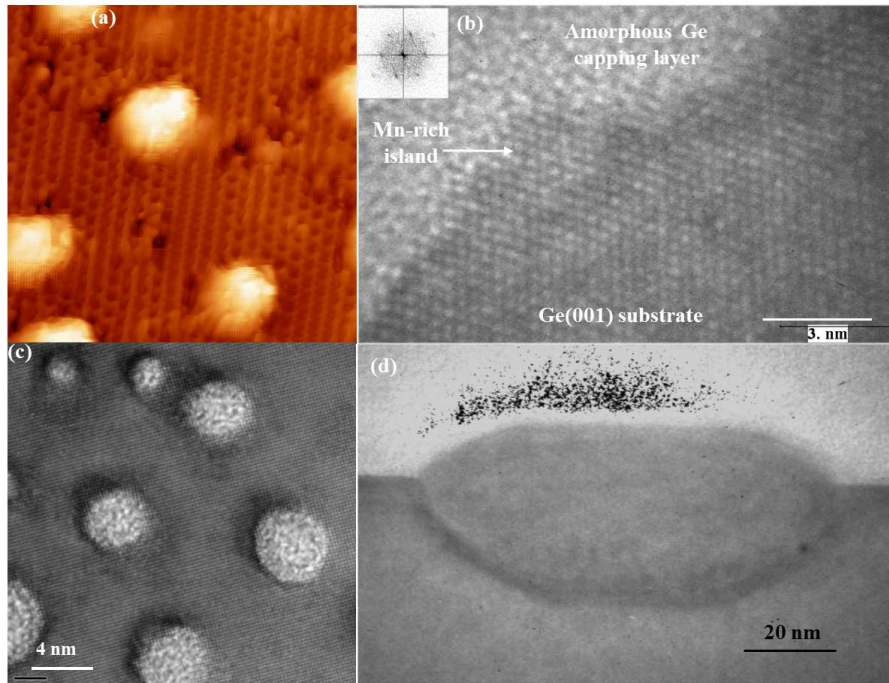


Figure 5: a) STM images showing the saturation size of Mn islands ( $V_s = -1.5\text{mV}$ ;  $I = 0.6\text{nA}$ ). b) HR-TEM image, in cross section mode of a Mn-rich island. Inset: Fourier transform of  $512 \times 512$  pixels centered on the Mn-rich island. c) Plane view HR-TEM image of nanocolumns. d)  $\text{Mn}_5\text{Ge}_3$  nanoislands formed after annealing a  $4 \text{ \AA}$ -thick Mn layer grown on Ge(001).

## Conclusion

This comprehensive study describes the initial stages of Mn growth in Ge(001) at  $(353 \pm 5)$  K. From the early step of the deposition, Mn atoms aggregate in small clusters. These findings corroborate with the numerous studies reporting on the difficulties of obtaining homogeneous  $\text{Ge}_{1-x}\text{Mn}_x$  DMS thin films by codepositing Mn and Ge on Ge(001). In this system, surface diffusion and Mn-pair interactions are the driving phenomena leading to the formation of monosized nanoislands as the Mn coverage increases to  $(0.65 \pm 0.05)$  ML. The formation of such a nanostructure follows a well-defined sequence. First, small islands are nucleated in the trench between two adjacent dimer rows. Most probably, these nuclei result from a reaction of surrounding Ge dimers with Mn adsorbed in the most favorable sites, namely the subsurface  $I_0$  and the surface  $H$  sites. As the Mn coverage increases, Ostwald ripening occurs resulting in an even distribution of Mn-rich nanoislands with a diameter of 4-5 nm and separated by a distance of 7-8 nm. This spatial distribution is very similar to the in-plane distribution of Mn-rich nanocolumns grown at 373 K, demonstrating that their morphology is determined at the very early stage of the growth when Mn atoms reach the Ge(001) surface. The nanocolumns characteristics with their resulting structural and magnetic properties can therefore be tuned by controlling the growth protocol, opening new routes for designing new nanostructures during growth.

## Acknowledgement

The authors thank D. Chaudanson for the technical support during the HR-TEM measurements and S. Giorgio for the fruitful discussions on the TEM images analysis.

## References

- (1) Wolf, S. A.; Awschalom, D. D.; Buhrman, R. A.; Daughton, J. M.; von Molnar, S.; Roukes, M. L.; Chtchelkanova, A.; Treger, D. M. Spintronics: a spin-based electronics vision for the future. *Science* **2001**, *294*, 1488.
- (2) Ohno, H. Making nonmagnetic semiconductors ferromagnetic. *Science* **1998**, *281*, 951.
- (3) Woodbury, H. H.; Tyler, W. W. Properties of Germanium Doped with Manganese. *Phys. Rev.* **1955**, *100*, 659.
- (4) Park, Y.; Hanbicki, S. C.; Erwin, S. C.; Hellberg, J. M.; Sullivan, J. M.; Mattson, J. E.; Ambrose, T. F.; Wilson, A.; Spanos, G.; Jonker, B. T. A group-IV ferromagnetic semiconductor:  $\text{Mn}_x\text{Ge}_{1-x}$ . *Science* **2002**, *295*, 651.
- (5) Fukushima, T.; Sato, K.; Katawama-Yoshida, H.; Dederichs, P. H. Spinodal Decomposition under Layer by Layer Growth Condition and High Curie Temperature Quasi-One-Dimensional Nano-Structure in Dilute Magnetic Semiconductors. *Jpn. J. Appl. Phys.* **2006**, *45*, L416.
- (6) Zeng, C.; Zhang, Z.; van Bentem, K.; Chisholm, M. F.; Weiering, H. H. Optimal doping control of magnetic semiconductors via subsurfactant epitaxy. *Phys. Rev. Lett.* **2008**, *100*, 066101.
- (7) Prabhakarana, K.; Ogino, T.; Hull, R.; Bean, J.; Peticolas, L. An efficient method for cleaning Ge(100) surface. *Surface Science* **1994**, *316*, L1031.
- (8) Schlier, R. E.; Farnsworth, H. E. Structure and Adsorption Characteristics of Clean Surfaces of Germanium and Silicon. *J. Chem. Phys.* **1959**, *30*, 917.
- (9) Kevan, S. Surface states and reconstruction on Ge(001). *Phys. Rev. B* **1985**, *32*, 2344.

- (10) Yang, W. S.; Wang, X. D.; Cho, K.; Kishimoto, J.; Fukatsu, S.; Hashizume, T.; Sakurai, T. Missing-dimer complexes and dimers on the Ge(001) surface. *Phys. Rev. B* **1994**, *50*, 2406.
- (11) Li, A. P.; Shen, J.; Thompson, J. R.; Weitering, H. H. Ferromagnetic percolation in  $\text{Mn}_x\text{Ge}_{1-x}$  dilute magnetic semiconductor. *Appl. Phys. Lett.* **2005**, *86*, 152507.
- (12) Zeng, C.; Zhu, W.; Erwin, S. C.; Zhang, Z.; Weitering, H. H. Initial stages of Mn adsorption on Ge(111). *Phys. Rev. B* **2004**, *70*, 205340.
- (13) Kuang, A.; Yuan, H.; Chen, H. First-principles study of manganese adsorption on Si(1 0 0) surface. *Applied Surface Science* **2009**, *255*, 6624.
- (14) Peng, G.; Huan, A.; Tok, E. S.; Feng, Y. P. Adsorption and diffusion of Co on the Si(001) surface. *Phys. Rev. B* **2006**, *74*, 195335.
- (15) Zhu, W.; Wetering, H. H.; Wang, E. G.; Kaxiras, E.; Zhang, Z. Contrasting Growth Modes of Mn on Ge(100) and Ge(111) Surfaces: Subsurface Segregation versus Inter-mixing. *Phys. Rev. Lett.* **2004**, *93*, 126102.
- (16) Dalpian, G. M.; da Silva, A. J. R.; Fazzio, A. Theoretical investigation of a possible  $\text{Mn}_x\text{Si}_{1-x}$  ferromagnetic semiconductor. *Phys. Rev. B* **2003**, *68*, 113310.
- (17) Hortamani, M.; Wu, H.; Kratzer, P.; Scheffler, M. Epitaxy of Mn on Si(001): Adsorption, surface diffusion, and magnetic properties studied by density-functional theory. *Phys. Rev. B* **2006**, *74*, 205305.
- (18) Wang, C., Jian-Tao and Chen; Wang, E.; Kawazoe, Y. Magic Monatomic Linear Chains for Mn Nanowire Self-Assembly on Si(001). *Phys. Rev. Lett.* **2010**, *105*, 116102.
- (19) Villarreal, R.; Longobardi, S., M. and Kster; Kirkham, C.; Bowler, D.; Renner, C. Structure of Self-Assembled Mn Atom Chains on Si(001). *Phys. Rev. Lett.* **2015**, *115*, 256104.

- (20) Choi, J.; Kyung, D.; Kim, Y.; Kim, D. H.; Kim, S. Creation and annihilation of single atom vacancy during subsurface diffusion. *Phys. Rev. B* **2010**, *82*, 201305(R).
- (21) Nolph, C.; Kassim, J.; Floro, J.; Reinke, P. Addition of Mn to Ge quantum dot surfaces—interaction with the Ge QD 105 facet and the Ge(001) wetting layer. *J Phys Condens Matter*. **2013**, *25*, 315801.
- (22) Stroppa, A.; Kresse, A., G. and Continenza Revisiting Mn-doped Ge using the Heyd-Scuseria-Ernzerhof hybrid functional. *Phys. Rev. B* **2011**, *83*, 085201.
- (23) Zandvliet, H. J.; van Houselt, A.; Hegeman, P. E. Embedded Co islands on Ge(001). *Surface Science* **2011**, *605*, 1129.
- (24) Gurlu, O.; Adam, O.; Zandvliet, H.; Poelsema, B. Self-organized, one-dimensional Pt nanowires on Ge(001). *Appl. Phys. Lett.* **2003**, *83*, 4610.
- (25) Necas, D.; Klapetek, P. Gwyddion: an open-source software for SPM data analysis. *Cent. Eur. J. Phys.* **2012**, *10*, 181.
- (26) Bihler, C.; Jaeger, C.; Vallaitis, T.; Gjukic, M.; Brandt, M. S.; Pippel, E.; Woltersdorf, J.; Gosele, U. Structural and magnetic properties of  $Mn_5Ge_3$  clusters in a dilute magnetic germanium matrix. *Applied Physics Letters* **2006**, *88*, 112506.
- (27) De Padova, P.; Ayoub, J.-P.; Berbezier, I.; Perfetti, P.; Quaresima, C.; Testa, A. M.; Fiorani, D.; Olivieri, B.; Mariot, J.-M.; Taleb-Ibrahimi, A.; Richter, M. C.; Heckmann, O.; Hricovini, K.  $Mn_{0.06}Ge_{0.94}$  diluted magnetic semiconductor epitaxially grown on Ge(001): Influence of  $Mn_{5x}Ge_3$  nanoscopic clusters on the electronic and magnetic properties. *Phys. Rev. B* **2008**, *77*, 045203.
- (28) Biegger, E.; Staheli, L.; Fonin, M.; Rudiger, U.; Dedkov, Y. S. Intrinsic ferromagnetism versus phase segregation in Mn-doped Ge. *Journal of Applied Physics* **2007**, *101*, 103912.

- (29) Sugahara, S.; Lee, K. L.; Yada, S.; Tanaka, M. Precipitation of Amorphous Ferromagnetic Semiconductor Phase in Epitaxially Grown Mn-doped Ge Thin Film. *Japanese Journal of Applied Physics* **2005**, *44*, L1426–L1429.
- (30) Ahlers, S.; Bougeard, D.; Riedl, H.; Abstreiter, G.; Trampert, A.; Kipferl, W.; Sperl, M.; Bergmaier, A.; Dollinger, G. Ferromagnetic Ge(Mn) nanostructures. *Physica E: Low-dimensional Systems and Nanostructures* **2006**, *32*, 422 – 425, Proceedings of the 12th International Conference on Modulated Semiconductor Structures.
- (31) Bougeard, D.; Ahlers, S.; Trampert, A.; Sircar, N.; Abstreiter, G. Clustering in a Precipitate-Free GeMn Magnetic Semiconductor. *Phys. Rev. Lett.* **2006**, *97*, 237202.
- (32) Jamet, M.; Barski, A.; Devillers, T.; Poydenot, V.; Dujardin, R.; Bayle-Guillemaud, P.; Rothman, J.; Bellet-Amalric, E.; Marty, A.; Cibert, J.; Mattana, R.; Tatarenko, S. High-Curie-temperature ferromagnetism in self-organized  $\text{Ge}_{1-x}\text{Mn}_x$  nanocolumns. *Nat. Mater.* **2006**, *5*, 653.
- (33) Devillers, T.; Jamet, M.; Barski, A.; Poydenot, V.; Bayle-Guillemaud, P.; Bellet-Amalric, E.; Cherifi, S.; Cibert, J. Structure and magnetism of self-organized  $\text{Ge}_{1-x}\text{Mn}_x$  nanocolumns on Ge(001). *Phys. Rev. B* **2007**, *76*, 205306.
- (34) Le, T.-G.; Nam, M.-T., D. N. H. and Dau; Luong, T. K. P.; Khiem, N. V.; Le Thanh, V.; Michez, L.-A.; Derrien, J. The effects of Mn concentration on structural and magnetic properties of  $\text{Ge}_{1-x}\text{Mn}_x$  diluted magnetic semiconductors. *J. Phys.: Conf. Ser.* **2011**, *292*, 012012.
- (35) Dalmas de Rotier, P.; Prestat, E.; Bayle-Guillemaud, P.; Boukhari, M.; Barski, A.; Marty, A.; Jamet, M.; Suter, A.; Prokscha, T.; Salman, Z.; Morenzoni, E.; Yaouanc, A. Core-shell nanostructure in a  $\text{Ge}_{0.9}\text{Mn}_{0.1}$  film observed via structural and magnetic measurements. *Phys. Rev. B* **2015**, *91*, 245408.

- (36) Arras, E.; Lancon, F.; Slipukhina, I.; Prestat, E.; Rovezzi, M.; Tardif, S.; Titov, A.; Bayle-Guillemaud, P.; d'Acapito, F.; Barski, A.; Favre-Nicolin, V.; Jamet, M.; Cibert, J.; Pochet, P. Interface-driven phase separation in multifunctional materials: The case of the ferromagnetic semiconductor GeMn. *Phys. Rev. B* **2012**, *85*, 115204.
- (37) Olive-Mendez, S.; Michez, L.; Spiesser, A.; Le Thanh, V. Epitaxial growth of strained Mn<sub>5</sub>Ge<sub>3</sub> nanoislands on Ge(001). *Phys. Status Solidi B* **2015**, *252*, 1854.
- (38) He, Z.; Smith, D. J.; Bennett, P. Endotaxial Silicide Nanowires. *Phys. Rev. Lett.* **2004**, *93*, 256102.
- (39) Bennett, P.; He, Z.; Smith, D. J.; Ross, F. Endotaxial silicide nanowires: A review. *Thin Solid Films* **2011**, *519*, 8434.